International Journal of Solids and Structures 46 (2009) 1456–1463

Contents lists available at ScienceDirect

International Journal of Solids and Structures

journal homepage: www.elsevier.com/locate/ijsolstr

Analysis of a mode-I crack perpendicular to an imperfect interface

Xian-Ci Zhong [a,b], Xian-Fang Li [a,*], Kang Yong Lee [c]

[a] Institute of Mechanics and Sensor Technology, School of Civil Engineering and Architecture, Central South University, Changsha, Hunan 410083, China
[b] School of Mathematics and Information Science, Guangxi University, Nanning, Guangxi 530004, China
[c] School of Mechanical Engineering, Yonsei University, Seoul 120-749, South Korea

ARTICLE INFO

Article history:
Received 28 May 2008
Received in revised form 9 October 2008
Available online 6 December 2008

Keywords:
Stress intensity factors
Imperfect interface
Spring model
Fourier transform
Winkler foundation

ABSTRACT

The elastostatic problem of a mode-I crack embedded in a bimaterial with an imperfect interface is investigated. The crack is in proximity to and perpendicular to the imperfect interface, which is governed by linear spring-like relations. The Fourier transform is applied to reduce the associated mixed-boundary value problem to a singular integral equation with Cauchy kernel. By numerically solving the resulting equation, stress intensity factors near both crack tips are evaluated. Obtained results reveal that the stress intensity factors in the presence of the imperfect interface vary between that with a perfect interface and that with a completely debonding interface. Moreover, an increase in the interface parameters decreases the stress intensity factors. In particular, when crack approaches to the weakened interface closer, the stress intensity factors become larger for a sliding interface, and become larger or smaller for a Winkler interface, depending on the crack lying in a stiffer or softer material. The influences of the imperfection of the interface on the stress intensity factors for a bimaterial composed of aluminum and steel are presented graphically.

1. Introduction

Composite materials have excellent mechanical performances such higher strength, lower weight, etc. as compared to individual constituents. Since composite materials are commonly composed of a matrix and some reinforced phases, the interfacial property plays a significant role in transferring loads between the matrix and the reinforced phases. A very large number of papers have been published for analyzing the effects of a perfect interface on mechanical behavior. For example, the interaction of a crack or an inclusion and perfect interface has been investigated by researchers (see e.g. Zak and Williams, 1963; Erdogan, 1965; Swenson and Rau, 1970; Cook and Erdogan, 1972; Rice, 1988; Selvadurai, 1994;Remeo and Ballarini, 1995; Li and Fan, 2001; Shin et al., 2004; among others).

However, it is rather difficult to guarantee two dissimilar materials to be perfectly bonded. This is an ideal state, and in reality, interfacial imperfection is inevitable, since the misfit of material properties involved may give rise to local debonding in a microscale (Suresh and Needleman, 1989). To simulate such an imperfect interface, some researchers suggested a spring-like model (Benveniste, 1985; Hashin, 1991, 2002; Klarbring and Movchan, 1998; Antipov et al., 2001). That is, instead of usual interface continuity conditions of displacements and stresses, interface tractions are still continuous across the interface, while interface displacements are discontinuous, which have a jump satisfying a linear relation with associated interface tractions, namely

$$T_n^I = T_n^{II} = \beta_n(u_n^I - u_n^{II}), \tag{1}$$

$$T_t^I = T_t^{II} = \beta_t(u_t^I - u_t^{II}), \tag{2}$$

$$T_s^I = T_s^{II} = \beta_s(u_s^I - u_s^{II}), \tag{3}$$

where T and u stand for interface tractions and displacements, a quantity with the superscript I or II refers to that in material I or II, the subscripts n, t, s denote the normal, and two tangential directions with reference to a local orthogonal system at some point on the interface, and $\beta_n, \beta_t, \beta_s$ are three independent spring-like constants or interface parameters. It is clear that when one interface parameter (β_n, say) tends to infinity, both the traction and displacement along the same (normal) direction are continuous, indicating that the interface is perfect in this direction. Only when all three interface parameters tend to infinity, the imperfect interface reduces to a perfect interface.

Using the above-suggested spring-like imperfect interface model, a considerable amount of investigations have been made. In particular, Bui et al. (2000) studied imperfect interlaminar interfaces in laminated composites, and gave their influence of strain energy release rates based on a double cantilever beam model, and furthermore Nairn (2007) made numerical implementation of imperfect interfaces via using finite element analysis. For a fibre-reinforced elastic composite, the interfaces between the elastic matrix and inhomogeneity are usually described by imperfect

* Corresponding author. Tel.: +86 731 887 7750.
E-mail address: xfli@mail.csu.edu.cn (X.-F. Li).

0020-7683/$ - see front matter © 2008 Elsevier Ltd. All rights reserved.
doi:10.1016/j.ijsolstr.2008.11.015

Nomenclature

a	Abscissa coordinate at the left crack tip
c	Abscissa coordinate at the right crack tip
E^j	Young's modulus of material j
$g(x)$	dislocation density function
G^j	shear modulus of material j
$k(s,x)$	kernel of integral equation
K^L, K^R	stress intensity factors at the left and right crack tip
l	half-length of crack
u^j, v^j	displacement components of material j
$\beta_n, \beta_t, \beta_s$	interface parameters
κ^j	elastic constant of material j
λ	the ratio of the crack half-length to position, i.e. $(c-a)/(c+a)$
ν^j	Poisson's ratio of material j
σ_0	applied stress
$\sigma^j_{xx}, \sigma^j_{xy}, \sigma^j_{yy}$	stress components of material j

interfaces. Meguid and Wang (1999) dealt with the interaction of crack and imperfect interface when dynamic antiplane shear waves are applied. A circular and elliptical inclusion embedded in an infinite matrix with imperfect interfaces has been analyzed by Sudak et al. (1999) and Shen et al. (2000). The interaction of a screw dislocation with an imperfect interface between two dissimilar semi-infinite elastic media has been analyzed by Fan and Wang (2003). Recently, a screw dislocation located in an annular coating layer imperfectly bonded an inner circular inhomogeneity and an unbounded matrix has been further coped with by Wang et al. (2007). On the other hand, a crack situated at the imperfect interface has been considered by Lenci (2001), who found only the logarithmic stress singularity near the crack tips. Instead of the usual traction-free crack surface condition, Udea et al. (2006) applied the spring-like imperfect interface condition to reconsider the corresponding antiplane shear problem, and found that the stress singularity at the crack tips is no longer an inverse square-root singularity, but a singularity of power law governed by the interface parameters.

This paper aims at analyzing the interaction of a crack and an imperfect interface. Differing from previous works, the crack being studied here is assumed not to be at the interface, but in proximity to and perpendicular to the imperfect interface. Using the Fourier transform technique, the associated mixed-boundary value problem is reduced to a singular integral equation. Numerical results are presented for a typical bimaterial with an imperfect interface. The influences of interfacial imperfection on stress intensity factors near the crack tips are analyzed in detail.

2. Problem and model

Consider two bonded dissimilar isotropic elastic solids with an imperfect interface, which occupy the right and left half-planes, respectively, as shown in Fig. 1. For convenience, media *I* and *II* in $x>0$ and $x<0$ are marked with material *I* and material *II*, respectively. For such a two-dimensional problem, at the imperfect interface the linear spring-like relations reduce to

$$\sigma^I_{xx}(0,y)=\sigma^{II}_{xx}(0,y)=\beta_n\left[u^I(0,y)-u^{II}(0,y)\right], \tag{4}$$

$$\sigma^I_{xy}(0,y)=\sigma^{II}_{xy}(0,y)=\beta_t\left[v^I(0,y)-v^{II}(0,y)\right], \tag{5}$$

where β_n and β_t are the normal and tangential interface parameters, respectively, the dimension of which is Newton/metre^3. Hereafter, u^j and v^j are the non-vanishing elastic displacements; σ^j_{xx}, σ^j_{yy} and σ^j_{xy} are the components of stress; and a quantity with superscript j ($j=I$ or II) denotes that in material *I* or *II*, respectively. Clearly, when $\beta_n=\beta_t=0$, two materials are fully debonded, and when $\beta_n\to\infty$ and $\beta_t\to\infty$, the interface is perfectly bonded. Other two cases are $\beta_t=0,\ \beta_n\to\infty$, corresponding to a sliding interface, and $\beta_t=0,\ \beta_n>0$, corresponding to a Winkler interface, respectively.

For the sake of simplicity, the crack is assumed to be perpendicular to the interface, and embedded in material *I*, occupying the segment $a<x<c(c>a>0)$ of the *x*-axis. So the length of the crack is $2l=c-a$. Since of interest is the singular field near the crack tip, it suffices to consider the crack subjected to internal pressure, namely

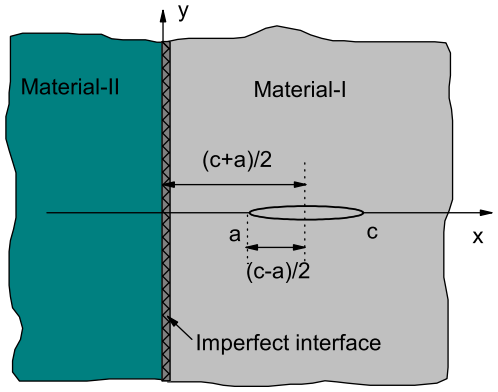

Fig. 1. A crack perpendicular to an imperfect interface in a bimaterial.

$$\sigma^I_{yy}(x,0)=-\sigma_0,\quad a<x<c. \tag{6}$$

For plane deformation, the associated constitutive equations are

$$\sigma^j_{xx}(x,y)=\frac{G^j}{\kappa^j-1}\left[(\kappa^j+1)\frac{\partial u^j}{\partial x}-(\kappa^j-3)\frac{\partial v^j}{\partial y}\right], \tag{7}$$

$$\sigma^j_{yy}(x,y)=\frac{G^j}{\kappa^j-1}\left[(\kappa^j+1)\frac{\partial v^j}{\partial y}-(\kappa^j-3)\frac{\partial u^j}{\partial x}\right], \tag{8}$$

$$\sigma^j_{xy}(x,y)=G^j\left(\frac{\partial v^j}{\partial x}+\frac{\partial u^j}{\partial y}\right), \tag{9}$$

where G^j is the shear modulus of material *j*, and in the above, $\kappa^j=3-4\nu^j$ for plane strain, while $\kappa^j=(3-\nu^j)/(1+\nu^j)$ for plane stress, ν^j the Poisson's ratio of material *j*. Furthermore, by using the equilibrium equations, the following differential equations can be easily derived:

$$\frac{\partial^2 u^j}{\partial x^2}+\frac{\kappa^j-1}{\kappa^j+1}\frac{\partial^2 u^j}{\partial y^2}+\frac{2}{\kappa^j+1}\frac{\partial^2 v^j}{\partial x\partial y}=0, \tag{10}$$

$$\frac{\partial^2 v^j}{\partial y^2}+\frac{\kappa^j-1}{\kappa^j+1}\frac{\partial^2 v^j}{\partial x^2}+\frac{2}{\kappa^j+1}\frac{\partial^2 u^j}{\partial x\partial y}=0, \tag{11}$$

where body forces have been neglected.

On the other hand, because of the symmetry of the problem, it is sufficient to determine elastic field in the upper half-plane of two bonded dissimilar materials, i.e. $y>0$. Therefore, in addition to (6), the boundary conditions are easily written as

$$\sigma^I_{xy}(x,0)=0,\quad 0<x<\infty, \tag{12}$$

$$v^I(x,0)=0,\quad 0<x<a,\quad c<x<\infty, \tag{13}$$

$$\sigma^{II}_{xy}(x,0)=0,\quad v^{II}(x,0)=0,\quad -\infty<x<0, \tag{14}$$

for a pressurized crack.

3. Procedure of solution

In order to solve the boundary value problem posed by mode-I crack embedded in a two-phase material with an imperfect interface, following Li (2006), we take elastic displacements u^j and v^j in terms of the following Fourier integrals:

$$u^j(x,y)=\int_0^\infty\left[A_1^j(\xi)+B_1^j(\xi)\xi y\right]e^{-y\xi}\sin(\xi x)d\xi+\int_0^\infty\left[A_2^j(\xi)+B_2^j(\xi)\xi x\right]e^{-\delta^j x\xi}\cos(\xi y)d\xi, \tag{15}$$

$$v^j(x,y)=\int_0^\infty\left[A_1^j(\xi)+\kappa^j B_1^j(\xi)+B_1^j(\xi)\xi y\right]e^{-y\xi}\cos(\xi x)d\xi+\int_0^\infty\left[\delta^j A_2^j(\xi)-\kappa^j B_2^j(\xi)+\delta^j B_2^j(\xi)\xi x\right]e^{-\delta^j x\xi}\sin(\xi y)d\xi, \tag{16}$$

where $\delta^I=1$ and $\delta^{II}=-1$, $A_{1,2}^j(\xi)$ and $B_{1,2}^j(\xi)$ are unknowns to be solved. From (7)–(9), expressions for the stress components can be calculated as follows:

$$\sigma_{xx}^j(x,y)=G^j\int_0^\infty\left[2A_1^j(\xi)+(\kappa^j-3)B_1^j(\xi)+2B_1^j(\xi)\xi y\right]\xi e^{-y\xi}\times\cos(\xi x)d\xi-G^j\int_0^\infty\left[2\delta^j A_2^j(\xi)-(\kappa^j-1)B_2^j(\xi)+2\delta^j B_2^j(\xi)x\xi\right]\xi e^{-\delta^j x\xi}\cos(\xi y)d\xi, \tag{17}$$

$$\sigma_{yy}^j(x,y)=-G^j\int_0^\infty\left[2A_1^j(\xi)+(\kappa^j+1)B_1^j(\xi)+2B_1^j(\xi)\xi y\right]\xi e^{-y\xi}\times\cos(\xi x)d\xi+G^j\int_0^\infty\left[2\delta^j A_2^j(\xi)-(\kappa^j+3)B_2^j(\xi)+2\delta^j B_2^j(\xi)x\xi\right]\xi e^{-\delta^j x\xi}\cos(\xi y)d\xi, \tag{18}$$

$$\sigma_{xy}^j(x,y)=-G^j\left\{\int_0^\infty\left[2A_1^j(\xi)+(\kappa^j-1)B_1^j(\xi)+2B_1^j(\xi)\xi y\right]\xi e^{-y\xi}\times\sin(\xi x)d\xi+\int_0^\infty\left[2A_2^j(\xi)-(\kappa^j+1)\delta^j B_2^j(\xi)+2B_2^j(\xi)x\xi\right]\xi e^{-\delta^j x\xi}\sin(\xi y)d\xi\right\}. \tag{19}$$

It is readily found that with the above expressions, the constitutive equations and equilibrium equations are automatically satisfied. The remaining is to seek elastic field, in particular near the crack tips via using appropriate boundary conditions in connection with interface conditions. To this end, it is natural to firstly determine the unknowns $A_{1,2}^j(\xi)$ and $B_{1,2}^j(\xi)$. From (12) and (14), one can obtain

$$A_1^{II}(\xi)=B_1^{II}(\xi)=0,\quad 2A_1^I(\xi)=(1-\kappa^I)B_1^I(\xi). \tag{20}$$

Then, application of interface condition (5) yields

$$2G^I A_2^I(\xi)-2G^{II}A_2^{II}(\xi)-G^I(\kappa^I+1)B_2^I(\xi)-G^{II}(\kappa^{II}+1)B_2^{II}(\xi)=0, \tag{21}$$

$$\int_0^\infty\left[\frac{\kappa^I+1}{2}+\xi y\right]B_1^I(\xi)e^{-y\xi}d\xi=-\int_0^\infty\left[\left(1+\frac{2G^I\xi}{\beta_t}\right)A_2^I(\xi)+A_2^{II}(\xi)-\left(\kappa^I+\frac{G^I\xi(\kappa^I+1)}{\beta_t}\right)B_2^I(\xi)+\kappa^{II}B_2^{II}(\xi)\right]\sin(\xi y)d\xi. \tag{22}$$

Using the conditions in (4) leads to

$$2G^{II}\xi A_2^{II}(\xi)+G^{II}(\kappa^{II}-1)\xi B_2^{II}(\xi)=\beta_n[A_2^I(\xi)-A_2^{II}(\xi)], \tag{23}$$

$$\int_0^\infty(-1+y\xi)B_1^I(\xi)\xi e^{-y\xi}d\xi=\int_0^\infty\left[\left(\xi+\frac{\beta_n}{2G^I}\right)A_2^I(\xi)-\frac{\beta_n}{2G^I}A_2^{II}(\xi)-\frac{(\kappa^I-1)\xi}{2}B_2^I(\xi)\right]\cos(\xi y)d\xi. \tag{24}$$

Now, the Fourier inverse transform is performed to Eqs. (22) and (24), and one gets

$$\left(1+\frac{2G^I\xi}{\beta_t}\right)A_2^I(\xi)+A_2^{II}(\xi)-\left(\kappa^I+\frac{G^I\xi(\kappa^I+1)}{\beta_t}\right)B_2^I(\xi)+\kappa^{II}B_2^{II}(\xi)=\omega_1, \tag{25}$$

$$\left(\xi+\frac{\beta_n}{2G^I}\right)A_2^I(\xi)-\frac{\beta_n}{2G^I}A_2^{II}(\xi)-\frac{(\kappa^I-1)\xi}{2}B_2^I(\xi)=\omega_2, \tag{26}$$

with

$$\omega_1=-\frac{2}{\pi}\int_0^\infty\left[\frac{\kappa^I+1}{2}\frac{\xi}{\xi^2+\eta^2}+\frac{2\xi\eta^2}{(\xi^2+\eta^2)^2}\right]B_1^I(\eta)d\eta, \tag{27}$$

$$\omega_2=\frac{2}{\pi}\int_0^\infty\left[-\frac{\eta^2}{\xi^2+\eta^2}+\frac{\eta^2(\eta^2-\xi^2)}{(\eta^2+\xi^2)^2}\right]B_1^I(\eta)d\eta, \tag{28}$$

where known identities (A1) and (A2), given in Appendix A, have been used.

According to Eqs. (21), (23), (25) and (26), the unknown functions $A_2^I(\xi)$, $A_2^{II}(\xi)$, $B_2^I(\xi)$ and $B_2^{II}(\xi)$ can be then expressed in terms of ω_1 and ω_2, i.e.

$$\begin{bmatrix}A_2^I(\xi)\\A_2^{II}(\xi)\\B_2^I(\xi)\\B_2^{II}(\xi)\end{bmatrix}=\begin{bmatrix}2G^I & -2G^{II} & -G^I(\kappa^I+1) & -G^{II}(\kappa^{II}+1)\\ -\beta_n & \beta_n+2G^{II}\xi & 0 & G^{II}(\kappa^{II}-1)\xi\\ 1+\frac{2G^I\xi}{\beta_t} & 1 & -\left(\kappa^I+\frac{G^I\xi(\kappa^I+1)}{\beta_t}\right) & \kappa^{II}\\ \xi+\frac{\beta_n}{2G^I} & -\frac{\beta_n}{2G^I} & -\frac{(\kappa^I-1)\xi}{2} & 0\end{bmatrix}^{-1}\begin{bmatrix}0\\0\\\omega_1\\\omega_2\end{bmatrix}=\begin{bmatrix}M_1^I(\xi)\\M_1^{II}(\xi)\\N_1^I(\xi)\\N_1^{II}(\xi)\end{bmatrix}\omega_1+\begin{bmatrix}M_2^I(\xi)\\M_2^{II}(\xi)\\N_2^I(\xi)\\N_2^{II}(\xi)\end{bmatrix}\omega_2, \tag{29}$$

where the detailed expressions for $M_{1,2}^j(\xi)$ and $N_{1,2}^j(\xi)$ are omitted here.

Inserting the above results in (29) into the expressions (17)–(19) for the stress components, and applying (6) and (13), we obtain triple integral equations as follows:

$$\int_0^\infty B_1^I(\xi)\cos(\xi x)d\xi=0,\quad 0<x<a,\quad c<x<\infty, \tag{30}$$

$$\int_0^\infty B_1^I(\xi)\xi\cos(\xi x)d\xi-\int_0^\infty\left\{\left[M_1^I(\xi)+\left(-\frac{\kappa^I+3}{2}+x\xi\right)N_1^I(\xi)\right]\omega_1+\left[M_2^I(\xi)+\left(-\frac{\kappa^I+3}{2}+x\xi\right)N_2^I(\xi)\right]\omega_2\right\}\xi e^{-x\xi}d\xi=\frac{\sigma_0}{2G^I},\quad a<x<c. \tag{31}$$

The explicit solution of Eqs. (30) and (31) seems hardly to obtain. In what follows, we convert the above triple integral equations to a singular integral equation with Cauchy kernel, and then give the numerical solution of the resulting singular integral equation. To this end, we define a new auxiliary dislocation density function $g(x)$ such that

$$g(x)=\frac{2}{1+\kappa^I}\frac{\partial v^I(x,0)}{\partial x}, \tag{32}$$

where the coefficient $2/(1+\kappa^I)$ is introduced for convenience. Taking into account (16) as well as (20) we have

$$v^I(x,0)=\frac{1+\kappa^I}{2}\int_0^\infty B_1^I(\xi)\cos(\xi x)d\xi,$$

and then (32) becomes

$$g(x)=-\int_0^\infty B_1^I(\xi)\xi\sin(\xi x)d\xi. \tag{33}$$

In view of $v^I(a,0) = v^I(c,0) = 0$, $g(x)$ is found to satisfy the following single-value displacement constraint condition

$$\int_a^c g(x)dx = 0. \tag{34}$$

Furthermore, performing the Fourier inverse transform to (33), $B_1^I(\xi)$ has the following integral representation:

$$B_1^I(\xi) = -\frac{2}{\pi\xi}\int_a^c g(s)\sin(\xi s)ds. \tag{35}$$

Substituting (35) into (31) and recalling the well-known identities (A3)–(A5), after some computations we get a singular integral equation with Cauchy kernel of the first kind, i.e.

$$\frac{1}{\pi}\int_a^c \frac{g(s)}{s-x}ds + \frac{1}{\pi}\int_a^c g(s)k(s,x)ds = -\frac{\sigma_0}{2G^I}, \quad a < x < c, \tag{36}$$

with

$$k(s,x) = \frac{1}{s+x} + \int_0^\infty \left\{\left[M_1^I(\xi) + \left(-\frac{\kappa^I+3}{2} + x\xi\right)N_1^I(\xi)\right](2s\xi - 1 - \kappa^I) + 2s\xi^2\left[M_2^I(\xi) + \left(-\frac{\kappa^I+3}{2} + x\xi\right)N_2^I(\xi)\right]\right\}e^{-(s+x)\xi}d\xi. \tag{37}$$

From the above analysis, it is found that a singular term is extracted and the kernel $k(s,x)$ becomes continuous. Clearly, it seems unlikely to obtain the closed-form solution to Eq. (36) unless $k(s,x)$ takes quite simple expressions for special situations. For a general case, introducing dimensionless variables as follows:

$$x = \frac{c-a}{2}\bar{x} + \frac{c+a}{2}, \quad s = \frac{c-a}{2}\bar{s} + \frac{c+a}{2}, \quad g(s) = \frac{\sigma_0}{2G^I}\bar{g}(\bar{s}), \tag{38}$$

we can write Eq. (36) as

$$\frac{1}{\pi}\int_{-1}^1 \frac{\bar{g}(\bar{s})}{\bar{s}-\bar{x}}d\bar{s} + \frac{1}{\pi}\int_{-1}^1 \bar{g}(\bar{s})\bar{k}(\bar{s},\bar{x})d\bar{s} = -1, \quad -1 < \bar{x} < 1, \tag{39}$$

where

$$\bar{k}(\bar{s},\bar{x}) = \frac{c-a}{2}k(s,x).$$

Furthermore, from a physical viewpoint, the inverse square-root singularity at the crack tips allows us to conveniently choose $\bar{g}(\bar{s})$ in the form

$$\bar{g}(\bar{s}) = \frac{f(\bar{s})}{\sqrt{1-\bar{s}^2}}, \tag{40}$$

where $f(\bar{s})$ is a bounded continuous function in $|\bar{s}| \leqslant 1$. Consequently, the closed Lobatto–Chebyshev collocation method is used to discretize the singular integral Eq. (39) into a system of linear algebraic equations

$$\frac{1}{n}\sum_{i=0}^n \lambda_i \frac{f(\bar{s}_i)}{\bar{s}_i - \bar{x}_m} + \frac{1}{n}\sum_{i=0}^n \lambda_i \bar{k}(\bar{s}_i,\bar{x}_m)f(\bar{s}_i) = -1, \quad m = 1,2,\ldots,n, \tag{41}$$

where $\bar{x}_m = \cos[(2m-1)\pi/(2n)]$, $m = 1,2,\ldots,n$; $\bar{s}_i = \cos(i\pi/n), i = 0,1,2,\ldots,n$; $\lambda_0 = \lambda_n = 1/2$, $\lambda_1 = \cdots = \lambda_{n-1} = 1$. In addition, the constraint condition (34) can be rewritten below

$$\sum_{i=0}^n \lambda_i f(\bar{s}_i) = 0. \tag{42}$$

Once the solution to linear algebraic Eqs. (41) and (42) is determined, the crack tip field will be obtained easily.

From the viewpoint of fracture mechanics, stress intensity factor is a very important parameter characterizing the stress field around crack tip. For the present study, we define the stress intensity factors near the right and left crack tips as follows:

$$K^L = \lim_{x\to a^-}\sqrt{2\pi(a-x)}\sigma_{yy}^I(x,0), \quad K^R = \lim_{x\to c^+}\sqrt{2\pi(x-c)}\sigma_{yy}^I(x,0). \tag{43}$$

Using the expression (40), one can get

$$K^L = \sqrt{\pi l}\sigma_0 f(-1), \quad K^R = -\sqrt{\pi l}\sigma_0 f(1). \tag{44}$$

4. Results and discussions

In this section, numerical computations are carried out to examine the effects of the interface parameters on the stress intensity factors. Prior to a general consideration, it is expedient to consider two well-known cases.

Firstly, let us consider a special case where materials *I* and *II* are identical and bonded perfectly, i.e. $G^I = G^{II}$, $\kappa^I = \kappa^{II}$, $\beta_n \to \infty$ and $\beta_t \to \infty$. After some computations, we observe that

$$k(s,x) = 0. \tag{45}$$

Furthermore, the solution of the singular integral equation with Cauchy kernel (36) can be expressed explicitly as

$$g(x) = \frac{\sigma_0}{4G^I}\frac{(a+c)-2x}{\sqrt{(x-a)(c-x)}}. \tag{46}$$

With knowledge of (46), it is easy to calculate the stress intensity factors at the left and right crack tips as

$$K^L = K^R = \sqrt{\pi l}\sigma_0, \tag{47}$$

in agreement with the known results (see, e.g. Fan, 1978).

Secondly, we deal with a two-phase material with a fully debonded interface, i.e. $\beta_n = \beta_t = 0$. In this case, the kernel in (37) reduces to

$$k(s,x) = \frac{x-s}{(s+x)^2} + \frac{4xs}{(s+x)^3}. \tag{48}$$

Furthermore, with the aid of the above-suggested collocation method, the stress intensity factors at the left and right crack tips can be evaluated. Here, we consider an edge crack with $a = 0$ and $\beta_n = \beta_t = 0$. It is noted that in solving such an edge crack, the constraint condition (42) should be replaced by $f(-1) = 0$, which in fact means that the crack mouth has no singularity. When taking $n = 100$ in Eqs. (41), we obtain that $K^R/\sigma_0\sqrt{\pi l} = 1.5861$, or equivalently, $K^R/\sigma_0\sqrt{2\pi l} = 1.1215$, identical to the well-known result for an edge crack in a semi-infinite elastic plane (see e.g. Tada et al., 1973).

4.1. Sliding interface

Now, let us to consider another special case of $\beta_n \to \infty$ and $\beta_t = 0$, which implies that the interface is sliding freely along the *y*-axis. Moreover, the normal displacement is imposed to be continuous. Then, it is found that $k(s,x)$ simplifies to

$$k(s,x) = \frac{1}{s+x} + \left[\frac{4sx}{(s+x)^3} - \frac{2s}{(s+x)^2}\right]\frac{G^I(\kappa^{II}+1)}{G^I(\kappa^{II}+1) + G^{II}(\kappa^I+1)}. \tag{49}$$

It is clear that this kernel is dependent on all the material properties, and so are the desired stress intensity factors.

To illustrate the variation of the stress intensity factors, aluminum and steel are chosen in the following calculation. Their Young's moduli are 80.0 and 208 GPa, and Poisson's ratios are 0.33 and 0.3, respectively. Two cases of combination are investigated, and Case A means that crack lies in a softer material aluminum, and Case B means that the crack lies in a stiffer material steel. Under the assumption of plane strain, Fig. 2 shows the variation of

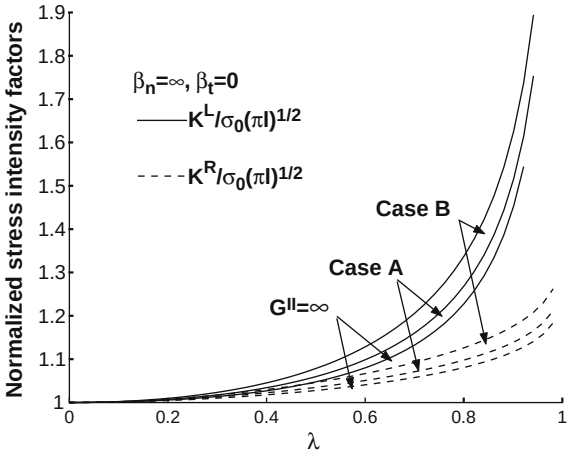

Fig. 2. The variation of the normalized stress intensity factors $K/\sigma_0\sqrt{\pi l}$ against the ratio λ for a sliding interface.

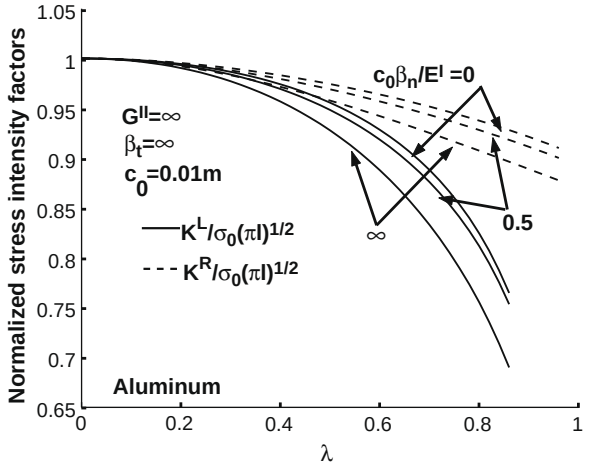

Fig. 3. The variation of the normalized stress intensity factors $K/\sigma_0\sqrt{\pi l}$ against the ratio λ for a crack in an elastic material resting on Winkler foundation.

normalized stress intensity factors $K/\sigma_0\sqrt{\pi l}$ on λ for Cases A and B, respectively. Hereafter, λ is chosen as the ratio $\lambda = (c-a)/(a+c)$. From Fig. 2, it is found that the normalized stress intensity factors increase with increasing λ. Or rather, the closer the distance between the crack and the sliding interface, the larger the stress intensity factors, which infers that a closer crack away from the sliding interface enhances crack growth. Moreover, as expected, the stress intensity factor near the left crack tip is greater than that near the right crack tip, implying that the left crack tip is easier to propagate than the right crack tip.

For comparison, we also depict the variation of the stress intensity factors when the crack-free material is a rigid solid in Fig. 2. For this case, $G^{II} \to \infty$ is required, and we then have

$$k(s,x) = \frac{1}{s+x}. \tag{50}$$

From Fig. 2, it is viewed that the corresponding stress intensity factors are least, compared to those for Cases A and B, irrespective of the left or right crack tip.

4.2. Winkler interface

Here, we turn our attention to a Winkler interface. In other words, we set $\beta_t \to \infty$ and so tangential displacement is continuous across the interface. In particular, if material *II* is rigid, $G^{II} \to \infty$, the interface collapses to the so-called Winkler foundation. For this case, numerical results are calculated and presented in Fig. 3. Different from the case of the sliding interface discussed in the previous subsection, for a cracked elastic material with a Winkler foundation, the stress intensity factors are found to decrease when the crack is close to the Winkler foundation. Moreover, the larger the normal interface parameter β_n, the smaller the stress intensity factors. This is in accordance with the observations given by Matysiak and Pauk (2003), who investigated the stress intensity factors of an edge crack in an elastic strip resting on Winkler foundation. In particular, when $\beta_n \to \infty$, the corresponding results reduce to those an elastic material perfectly bonded to a rigid foundation, and they are listed in Table 1, in exact agreement with those obtained by Isida (1970), who gave fitting approximate expressions for the stress intensity factors for this case based on numerical results obtained

$$K^L = \sigma_0\sqrt{\pi l}\left(1 - 0.175\lambda^2 - 0.245\lambda^3\right), \quad \lambda \leqslant 0.8, \tag{51}$$

$$K^R = \sigma_0\sqrt{\pi l}\left(1 - 0.145\lambda^2\right), \quad \lambda \leqslant 0.9. \tag{52}$$

Table 1
$K/\sigma_0\sqrt{\pi a}$ for an elastic material perfectly bonded to a stiffened edge.

λ	Left crack tip		Right crack tip	
	Present results	Isida (1970)	Present results	Isida (1970)
0	1.0000	1.0000	1.0000	1.0000
0.1	0.9977	0.9980	0.9979	0.9986
0.2	0.9904	0.9910	0.9922	0.9942
0.3	0.9771	0.9776	0.9832	0.9869
0.4	0.9568	0.9563	0.9716	0.9768
0.5	0.9278	0.9256	0.9578	0.9637
0.6	0.8879	0.8841	0.9422	0.9478
0.7	0.8330	0.8302	0.9253	0.9290
0.8	0.7552	0.7626	0.9075	0.9072
0.9	0.6328	–	0.8890	0.8825

According to these two formulae, evaluated results are also given in Table 1 for the purpose of comparison. It is readily found that the present results are rather satisfactory compared to the previous results.

On the other hand, if material *II* is another dissimilar elastic solid, the interface is assumed to be governed by a linear relation between the displacement jump and normal stress

$$\sigma^I_{xx}(0,y) = \sigma^{II}_{xx}(0,y) = \beta_n\left[u^I(0,y) - u^{II}(0,y)\right], \tag{53}$$

which looks like a spring. For such Winkler interface, the variation of the stress intensity factors is strongly reliant on the material properties of the other crack-free elastic medium, which can be observed in Fig. 4(a and b) for Cases A and B, respectively. Clearly, for the crack lying in the softer Al, the stress intensity factors are seen to drop down when the crack moves closer to the Winkler interface. This is not true for the crack lying in the stiffer steel, and trend is reversed for the latter. That is, when the distance between the crack and the Winkler interface is reduced, the stress intensity factors rise. As a consequence, for a crack lying in a softer material, it is safer when the crack is closer to the Winkler interface, whereas for a crack lying in a stiffer material, it is safer when the crack is farther to the Winkler interface. In other words, the Winkler interface can promote or impede crack propagation, depending on it lying in a harder or softer material, respectively.

4.3. The case of $\beta_n = \beta_t$

For the previous analysis, it is found that not only the interface parameters but also the material properties of two materials

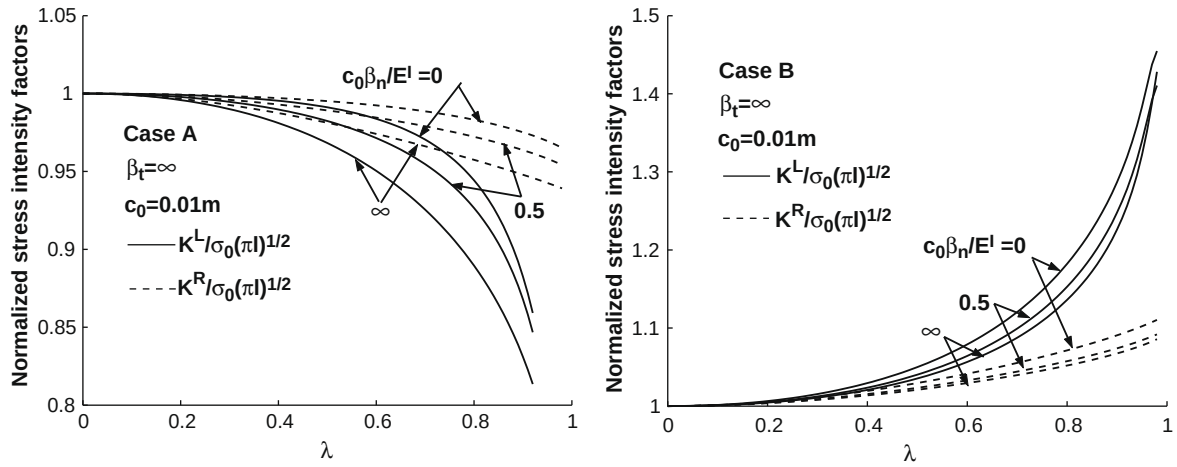

Fig. 4. The variation of the normalized stress intensity factors $K/\sigma_0\sqrt{\pi l}$ against the ratio λ for the case of Winkle interface; (a) crack lies in a softer material; (b) crack lies in a stiffer material.

strongly affect the stress intensity factors. Here, we consider a special case of $\beta_n = \beta_t$.

Fig. 5(a and b) illustrate the variation of the normalized stress intensity factors near the crack tips against the ratio λ for $c_0\beta_t/E^I = c_0\beta_n/E^I = 0, 0.5, \infty$ for Cases A and B, respectively, where $c_0 = (a+c)/2$ and E^I is the Young's modulus of material I. When $c_0\beta_t/E^I = c_0\beta_n/E^I = 0$, two materials are fully debonded, and from Fig. 5(a and b) the curves of $K^R/\sigma_0(\pi l)^{1/2}$ are in agreement with the corresponding ones given in Isida (1971). When $c_0\beta_t/E^I = c_0\beta_n/E^I \to \infty$, two materials are perfectly bonded (Remeo and Ballarini, 1995). For this case, with increasing λ, the normalized stress intensity factors decline for Case A and increase for Case B, respectively. This is similar to the trend when the imperfect interface is Winkler interface, as seen in Fig. 4(a and b). The phenomena reveal that when the crack is closer to the interface, crack growth will be impeded, or the path is kinked or unstable for the crack lying in a softer material (Case A), and enhanced or stable for the crack lying in a stiffer material (Case B), in agreement with the experimental observations (Suresh et al., 1992) for the growth of a crack approaching a perpendicularly-oriented bimaterial interface. Also, when two dissimilar materials are perfectly bonded, such similar trends have been confirmed for a crack embedded in a softer or a stiffer solid, respectively (Cook and Erdogan, 1972; Wang and Stable, 1998). Furthermore, for the case of $c_0\beta_t/E^I = c_0\beta_n/E^I = 0.5$, the curves of normalized stress intensity factors are always located between the curves corresponding to $c_0\beta_t/E^I = c_0\beta_n/E^I = 0$ and to $c_0\beta_t/E^I = c_0\beta_n/E^I = \infty$. It indicates that full debonding and perfect interface are indeed the limiting cases of the imperfect interface. It is interesting to note that for Case B, the normalized stress intensity factors always rise with an increase in the ratio λ, regardless of the values of β_t and β_n, while for Case A, the stress intensity factors remain unchanged for a certain finite value.

4.4. General case

Generally speaking, the interface of two bonded dissimilar materials is neither perfectly bonded nor completely debonding. That is to say, the interface parameters β_t and β_n can take various values. The influence of the imperfection of the interface on the stress intensity factor is shown in Fig. 6(a and b) for Cases A and B, respectively, where a specified crack geometry with $\lambda = 0.9$ and $a + c = 0.02m$ is considered. From Fig. 6(a and b) it is seen that an increase in both β_n and β_t decreases the normalized stress intensity factors, regardless of Cases A and B. In other words, for a fixed crack position, the stress intensity factors become larger if imperfection is enhanced: β_n or β_t declines. As a result, in order to avoid

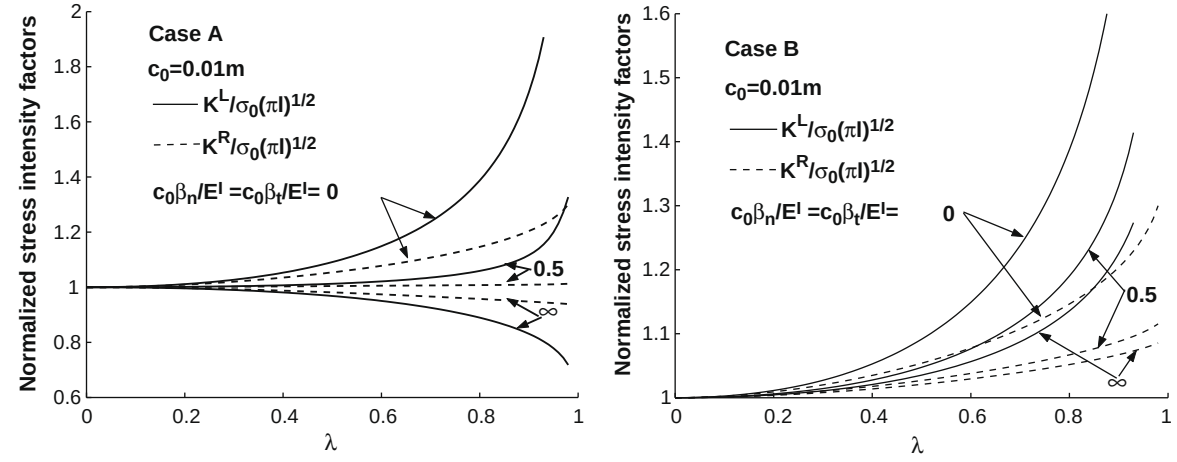

Fig. 5. The variation of the normalized stress intensity factors $K/\sigma_0\sqrt{\pi l}$ against the ratio λ when two interface parameters are equal: $\beta_n = \beta_t$, (a) crack lies in a softer material; (b) crack lies in a stiffer material.

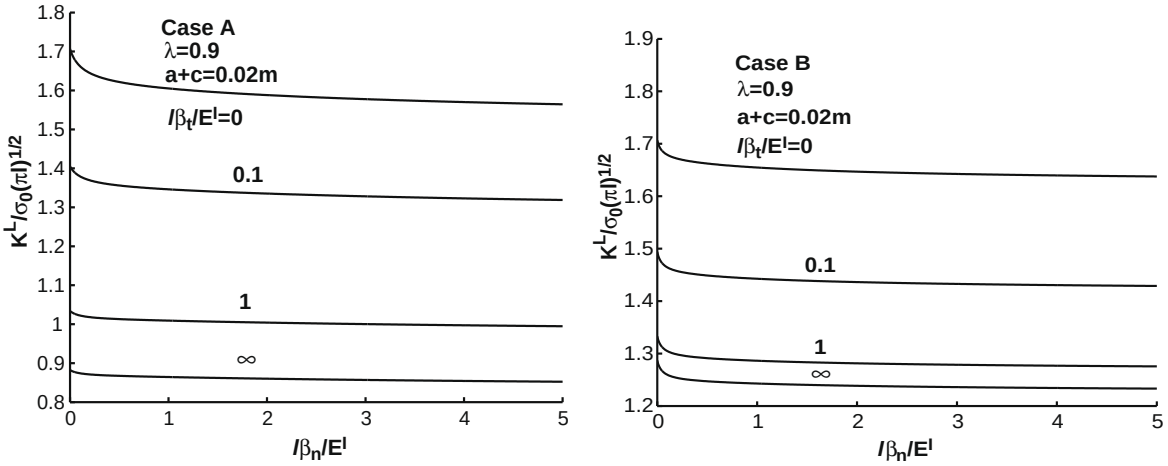

Fig. 6. The effects of the imperfection of the interface on the normalized stress intensity factors at the crack tip close to the imperfect interface $K/\sigma_0\sqrt{\pi l}$ when $\lambda = 0.9,\ a + c = 0.02m$, (a) crack lies in a softer material; (b) crack lies in a stiffer material.

crack advance, it is always desired that the interface is designed to be perfectly bonded together as possible as we can, since the stress intensity factors at both crack tips can be effectively reduced when β_n and/or β_t increase.

5. Conclusions

The analysis of the stress intensity factors for a crack perpendicular to an imperfect interface is made. In order to simulate the imperfection of the interface of two dissimilar elastic materials, a spring-like model with vanishing thickness is proposed. Applying the Fourier transform technique, the crack problem is reduced to solving singular integral equation. Then, by using the Lobatto–Chebyshev collocation method, the numerical results of the stress intensity factors near the left and right crack tips are obtained. The effects of the imperfect interface on the fracture parameter are demonstrated graphically. Some conclusions are drawn out as follows:

- An increase in the interface parameters β_n and β_t decreases the stress intensity factors for a fixed crack.
- Imperfection of the interface causes the stress intensity factors to vary between that with a completely debonding and that with a perfectly bonded interface.
- For a sliding interface, the closer a crack is away from the interface, the larger the stress intensity factors, irrespective of a crack lying in softer or stiffer materials.
- For a Winkler interface, with the distance of the crack and the interface decreasing, the stress intensity factors become smaller when the crack is situated in a softer material, and larger when the crack is situated in a stiffer material, respectively.

Acknowledgements

This work was supported by the National Natural Science Foundation of China under Grant No. 10672189, and supported by the China–Korea Binational Joint Research Program (No. 10711140645). The authors are grateful to two anonymous referees for their valuable comments and suggestions to improve the original manuscript.

Appendix A. Appendix

Some identities related to infinite integrals used in the present paper are listed as follows (Gradshteyn and Ryzhik, 1980):

$$\int_0^\infty e^{-y\eta}\sin(\xi y)dy = \frac{\xi}{\xi^2+\eta^2}, \int_0^\infty y e^{-y\eta}\sin(\xi y)dy = \frac{2\eta\xi}{(\xi^2+\eta^2)^2}, \quad \text{(A1)}$$

$$\int_0^\infty e^{-y\eta}\cos(\xi y)dy = \frac{\eta}{\xi^2+\eta^2}, \int_0^\infty y e^{-y\eta}\cos(\xi y)dy = \frac{\eta^2-\xi^2}{(\xi^2+\eta^2)^2} \quad \text{(A2)}$$

and

$$\frac{2}{\pi}\int_0^\infty \sin(s\xi)\cos(x\xi)d\xi = \frac{1}{\pi}\left(\frac{1}{s-x}+\frac{1}{s+x}\right), \quad \text{(A3)}$$

$$\int_0^\infty \frac{\sin(\eta s)}{(\eta^2+\xi^2)\eta}d\eta = \frac{\pi(1-e^{-\xi s})}{2\xi^2}, \int_0^\infty \frac{\eta\sin(\eta s)}{\eta^2+\xi^2}d\eta = \frac{\pi}{2}e^{-\xi s}, \quad \text{(A4)}$$

$$\int_0^\infty \frac{\eta\sin(\eta s)}{(\eta^2+\xi^2)^2}d\eta = \frac{\pi s}{4\xi}e^{-\xi s}. \quad \text{(A5)}$$

References

Antipov, Y.A., Avila-Pozos, O., Kolaczkowski, S.T., Movchan, A.B., 2001. Mathematical modal of delamination cracks on imperfect interfaces. Int. J. Solid. Struct. 38, 6665–6697.

Benveniste, Y., 1985. The effective mechanical behaviour of composite materials with imperfect contact between the constituents. Mech. Mater. 4, 197–208.

Bui, V.Q., Marechal, E., Nguyen-Dang, H., 2000. Imperfect interlaminar interfaces in laminated composites: interlaminar stresses and strain-energy release rates. Compos. Sci. Technol. 60, 131–143.

Cook, T.S., Erdogan, F., 1972. Stresses in bonded materials with a crack perpendicular to interface. Int. J. Eng. Sci. 10, 677–697.

Erdogan, F., 1965. Stress distribution in bonded dissimilar materials containing circular or ring-shaped cavities. J. Appl. Mech. 32, 829–836.

Fan, H., Wang, G.F., 2003. Screw dislocation interacting with imperfect interface. Mech. Mater. 35, 943–953.

Fan, T.Y., 1978. Foundation of Fracture Mechanics. Jiangsu Sci-Tech Press, Nanjing (in Chinese).

Gradshteyn, I.S., Ryzhik, I.M., 1980. Table of Integrals, Series and Products. Academic Press, New York.

Hashin, Z., 1991. Thermoelastic properties of particulate composites with imperfect interface. J. Mech. Phys. Solids 39, 745–762.

Hashin, Z., 2002. Thin interphase/imperfect interface in elasticity with application to coated fiber composites. J. Mech. Phys. Solids 50, 2509–2537.

Isida, M., 1971. Effect of width and length on stress intensity factors of internally cracked plates under various boundary conditions. Int. J. Fract. 7, 301–316.

Isida, M., 1970. On the determination of stress intensity factors for some common structural problems. Eng. Fract. Mech. 2, 61–79.

Klarbring, A., Movchan, A.B., 1998. Asymptotic modelling of adhesive joints. Mech. Mater. 28, 137–145.

Lenci, S., 2001. Analysis of a crack at a weak interface. Int. J. Fract. 108, 275–298.

Li, X.-F., Fan, T.-Y., 2001. The asymptotic stress field for a rigid circular inclusion at the interface of two bonded dissimilar elastic half-space materials. Int. J. Solids Struct. 38, 8019–8035.

Li, X.-F., 2006. T-stress near the tips of a cruciform crack with unequal arm. Eng. Fract. Mech. 73, 671–683.

Matysiak, S.J., Pauk, V.J., 2003. Edge crack in an elastic layer resting on Winkler foundation. Eng. Fract. Mech. 70, 2353–2361.
Meguid, S.A., Wang, X.D., 1999. Wave scattering from cracks and imperfectly bonded inhomogeneities in advanced materials. Mech. Mater. 31, 187–195.
Nairn, J.A., 2007. Numerical implementation of imperfect interfaces. Comp. Mater. Sci. 40, 525–536.
Remeo, A., Ballarini, R., 1995. A crack very close to a bimaterial interface. J. Appl. Mech. 63, 614–619.
Rice, J.R., 1988. Elastic fracture mechanics concepts for interfacial cracks. J. Appl. Mech. 55, 98–103.
Selvadurai, A.P.S., 1994. A unilateral contact problem for a rigid disc inclusion embedded between two dissimilar elastic half-spaces. Q. J. Mech. Appl. Math. 47, 493–510.
Shen, H., Schiavone, P., Ru, C.Q., Mioduchowski, A., 2000. An elliptic inclusion with imperfect interface in anti-plane shear. Int. J. Solids Struct. 37, 4557–4575.
Shin, K.C., Liu, H., Lee, J.J., Choi, S.T., 2004. Interfacial crack tip field in anisotropic/isotropic bimaterials. Compos. Struct. 66, 673–676.
Sudak, L.J., Ru, C.Q., Schiavone, P., Mioduchowski, A., 1999. A circular inclusion with inhomogeneously imperfect interface in plane elasticity. J. Elasticity 55, 19–41.
Suresh, S., Needleman, A., 1989. Interfacial Phenomena in Composites. Elsevier Applied Science, New York.
Suresh, S., Sugimura, Y., Tschegg, E.K., 1992. The growth of a fatigue crack approaching a perpendicularly-oriented, bimaterial interface. Scripta Metall. 27, 1189–1194.
Swenson, D.O., Rau, C.A., 1970. The stress distribution around a crack perpendicular to an interface between materials. Int. J. Fract. Mech. 6, 357–365.
Tada, H., Paris, P.C., Irwin, G.R., 1973. The Stress Analysis of Cracks Handbook. Del Research Corp., Hellertown, Pennsylvania.
Udea, S., Biwa, S., Watanabe, K., et al., 2006. On the stiffness of spring model for closed crack. Int. J. Eng. Sci. 44, 874–888.
Wang, X., Pan, E., Roy, A.K., 2007. New phenomena concerning a screw dislocation interacting with two imperfect interfaces. J. Mech. Phys. Solids 55, 2717–2734.
Wang, T.C., Stable, P., 1998. Stress state in front of a crack perpendicular to bimaterial interface. Eng. Fract. Mech. 59, 471–485.
Zak, A.R., Williams, M.L., 1963. Crack point stress singularities at a bi-material interface. J. Appl. Mech. 39, 142–143.